The Molecular Dynamics Study of Lithium Ion Conduction in Phosphate Glasses and the Role of Non-Bridging Oxygen

A. Karthikeyan,[†] P. Vinatier,[†] A. Levasseur,[†] and K. J. Rao[‡,*]

Institut de Chimie de la Matière Condensée de Bordeaux-CNRS et Ecole Nationale Supérieure de Chimie et de Physique de Bordeaux BP-108, F-33402 Talence Cedex, France, and Solid State and Structural Chemistry Unit, Indian Institute of Science, Bangalore 560 012, India

Received: January 19, 1999

Molecular dynamics (MD) simulation of lithium phosphate ($Li_2O-P_2O_5$) glasses with varying Li_2O content has been carried out. Two different P—O distances corresponding to phosphorus coordination with bridging oxygen (BO) and non-bridging oxygen (NBO) were identified in the simulated glasses. NBO−BO interconversion or bond switching was noted, which results in a dynamic equilibration of the tetrahedral phosphate units (P^n, $n = 1,3$ indicates the number of bridging oxygen atoms in the coordination of phosphorus). The NBO−BO bond switching is mildly activated with an effective activation barrier of 0.03−0.05 eV. Lithium ion jumps do not appear to be strongly coupled to bond switching. But the number of Li^+ ions coordinated to an optimum number of NBOs and the number of Li^+ ions jumping out of their sites appear to be correlated. Detailed analysis was made of the dynamics of P^n species and new insights have been obtained regarding ion migration in network-modified phosphate glasses.

Introduction

Alkali oxide−phosphorus pentoxide ($M_2O-P_2O_5$, where M is an alkali element) is a classical glass-forming system. The extensive quasi-two-dimensional polymeric network of P_2O_5 is known to be systematically depolymerized by the addition of a modifier like Li_2O.[1,2] As the ratio $R = Li_2O/P_2O_5$ in the glass is increased from 0 to 3, the glass composition courses through the stoichiometric meta- and pyrophosphates to the orthophosphates.[3−5] Glasses are, however, difficult to form in compositions where *R* values approach 3. Lithium phosphate glasses are also typical ionic conductors in which the conductivity is due exclusively to the transport of Li^+ ions. There have been several studies on the electrical transport behavior of lithium phosphate glasses over a wide range of compositions.[2,6] The activation barriers decrease significantly when *R* is increased and the conductivity increases by >3 orders of magnitude[6] as *R* is increased from about 0.1 to 1.5.

The depolymerization or modification caused by Li_2O results in converting bridging oxygens (BOs) to non-bridging oxygens (NBOs). The presence of NBOs has been established in silicate glasses by several experiments.[7−9] It is generally believed that in the glass structure, Li^+ ions are coordinated to 4 to 6 oxygens of which an unspecified number are NBOs. Further, it is generally assumed that during electrical transport, Li^+ ions jump between sites of almost similar energies and coordination geometries.[2,6] The frequency dependence of conductivity is considered to arise from jumps among such similar sites present near an NBO. Several models of ion transport, such as weak electrolyte model[10,11] and diffusion-controlled relaxation model,[12] assume a relatively permanent but random disposition of such NBOs in the glass structure. A significant departure from this assumption is evident in the work of Greaves and Ngai[13,14] whose approach suggests a dynamic rearrangement of the NBOs in network-forming silicates. Similar NBO dynamics are implied in magic-angle spinning nuclear magnetic resonance data on silicates.[15] Such dynamic rearrangements of NBOs have the implication that the Li^+ ion transport may be assisted by NBO−BO bond switching and the resulting coulombic disturbance. The mechanism has been imaginatively described as a 'catch and carry' process.[16] However, using elegant nuclear magnetic resonance (NMR) studies, Stebbins and co-workers have shown that in silicate melts, the NBO−BO bond switching is very slow and occurs with higher activation barriers that are comparable in magnitude to the activation barrier for shear flow. Lithium ion motion in these melts was not coupled to NBO−BO dynamics. Because the formation of NBOs is a common feature of all network glasses, such as those of alkali phosphates, it is necessary to examine if this imaginative and plausible mechanism of ion transport is operative in any of them. Formation of NBOs is the fundamental step in modification and is a paradigm of supreme importance to the physical chemistry of the glassy state. Therefore, the presence and the dynamics of NBOs need to be examined further.

Molecular dynamics (MD) simulation has been used in recent times very effectively to gain insight into important problems of the glassy state. For example, the mixed alkali effect in silicate glasses was shown to result from site and hence path selectivities of alkali ions.[17] Similarly, the Ag^+ ion motion in fast-ion-conducting $AgI-Ag_2MoO_4$ glasses was shown to involve only mixed (oxygen−halogen) coordinated sites.[18] In our earlier work, BO and NBO in simulated silicate glasses were identified using a distance criterion.[17] It should therefore be interesting to address the problem of NBOs and their dynamics in glasses by MD simulation.

Glasses of the formula $xLi_2O-(1-x)P_2O_5$ have been studied in this work by MD simulation. This system of glasses is very interesting, and has a potential for application as electrolytes in solid-state batteries. We have specifically addressed the

* Corresponding author.
† Institut de Chimie de la Matière Condensée de Bordeaux - C.N.R.S.
‡ Solid State and Structural Chemistry Unit.

10.1021/jp990228c CCC: $18.00
Published on Web 07/13/1999

TABLE 1: Potential Parameters and Number of Particles Used in the Simulation

parameter	Li	P	O
Z (e units)	0.6	3.0	−1.2
σ (Å)	1.8	1.74	2.84
composition		number of particles	
LP33	94	188	517
LP50	160	160	480
LP66	248	124	434

following questions in this work: (i) Is it possible to identify NBOs in a quantitatively satisfactory manner in MD simulation? (ii) Is there a dynamic rearrangement of NBOs in the glasses and therefore a dynamic equilibrium of corresponding phosphate species? (iii) Is there any influence of the dynamics of NBOs on Li^+ ion transport? Although the answers to all three questions are positive, the transport mechanism is not a simple 'catch and carry' by NBOs. Rather surprisingly, the NBO−BO dynamics appear to be very much faster than those in silicate glasses. The possible origin of this vital difference is also examined.

Methodology of Simulation

Three compositions of the lithium phosphate glasses of the general formula $xLiO_2 - (1 - x)P_2O_5$, with x = 0.33, 0.5, and 0.66, were chosen for MD simulation. The compositions were designated as LP33 (x = 0.33), LP50 (x = 0.50), and LP66 (x = 0.66), respectively. These glasses span the glass compositions widely investigated in experiments.[6] Born−Mayer type pair potential was used to calculate the potential energy and its derivative:

$$\phi_{ij} = (Z_i Z_j / r_{ij}) + A_{ij} \exp[(\sigma_{ij} - r_{ij})/\rho_{ij})] \qquad (1)$$

In eq 1, A_{ij}, σ_{ij}, and ρ_{ij} are the repulsive parameters for the interaction of i and j ions whose charges are Z_i and Z_j, respectively. Various aspects of this potential function have been described earlier.[17,18] Potential parameters used in the present study are listed in Table 1. The MD simulations were performed with a microcanonical ensemble (NEV) with ∼800 particles (exact numbers are given in Table 1). Experimental densities were used in the fixing box dimension at 300 K, whereas slightly lower densities were used at higher temperatures. The equations of motion were integrated using the fifth-order Gear predictor−corrector algorithm.[19] Initial simulation for homogeneous mixing of the system was carried out at 5000 K and then at 3000 K. The system was then cooled to 1000 K at the rate of 1 K/fs. Further cooling to 700 and 300 K was performed at the rate of 0.1 K/fs. At each temperature (1000, 700, and 300 K), the system was equilibrated for 30 ps and data were collected for the succeeding 50 ps. A time step of 1 fs was used in the simulations. For the computation of dynamic quantities, the coordinates were stored every 0.1 ps. At higher temperatures, trial density was used and for the room temperature (300 K) simulation, experimental density was employed. The pressure of the equilibrated system in all three compositions was less than ∼2 GPa. Simulations were also performed with formal charges on the ions instead of the adjusted charges given in Table 1. Although all other results were almost identical, the system pressures were unacceptably high. Therefore, results obtained with adjusted charges only are presented and discussed.

Results and Discussion

Structure of Simulated Glasses. The MD simulation results of the structures were examined first because several structural features are known from previous experimental studies. The important structural features are related to the presence of phosphate tetrahedra, lithium coordination, and intertetrahedral connectivities. The various pair distribution functions (PDFs) that have a direct bearing on these aspects are shown in Figure 1a−d. The interatomic distances, coordination numbers, and other relevant details obtained from the analysis of Figure 1a−d are listed in Table 2. The bond angle distribution (BAD) for O−P−O, P−O−P, O−Li−O, and O−O−O are shown in Figure 2a−d. All these values refer to the glasses equilibrated at 300 K. A common cutoff distance was used for the computation of both the coordination numbers and the BADs, and these distances are also listed in Table 2. The BADs were determined by first referencing the central atom and then defining the other two atoms that lie within the cutoff distances.

Two very clearly defined P−O distances are seen in Figure 1a in all three compositions of the simulated glasses. These two

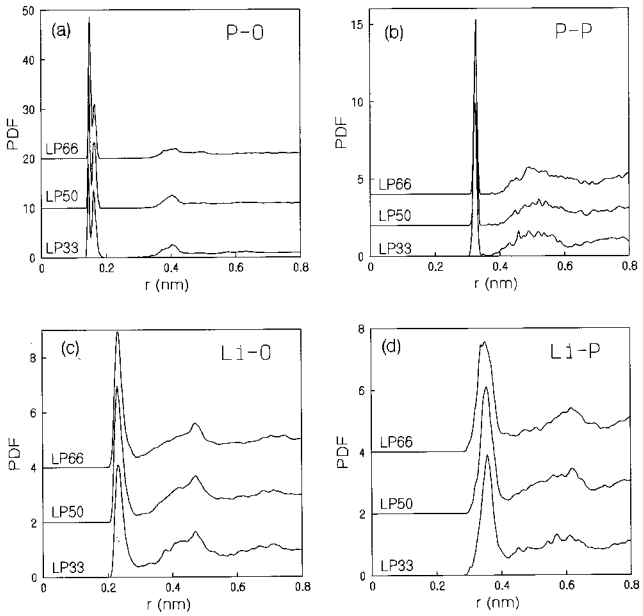

Figure 1. Pair distribution functions (PDF) at 300 K for the three glass compositions: (a) P−O; (b) P−P; (c) Li−O; and (d) Li−P.

TABLE 2: Pair Distances and Other Structural Parameters at 300 K

pair	composition	1st peak position, Å	coordination number	cutoff for coordination, Å
P−O (I peak)	LP33	1.45	1.52	1.525
	LP50	1.47	1.92	1.550
	LP66	1.50	2.51	1.575
P−O (II peak)	LP33	1.62	2.48	2.275
	LP50	1.62	2.08	1.875
	LP66	1.62	1.49	1.875
O−O	LP33	2.55	4.41	2.800
	LP50	2.55	4.01	2.825
	LP66	2.55	3.43	2.850
P−P	LP33	3.25	2.52	3.425
	LP50	3.27	2.15	3.425
	LP66	3.25	1.58	3.425
Li−Li	LP33	3.00	2.20	4.050
	LP50	3.00	3.41	4.075
	LP66	3.00	6.21	4.075
Li−P	LP33	3.57	4.33	4.075
	LP50	3.55	3.45	4.075
	LP66	3.50	3.35	4.075
Li−O	LP33	2.35	3.82	2.800
	LP50	2.35	3.63	2.800
	LP66	2.35	3.40	2.800

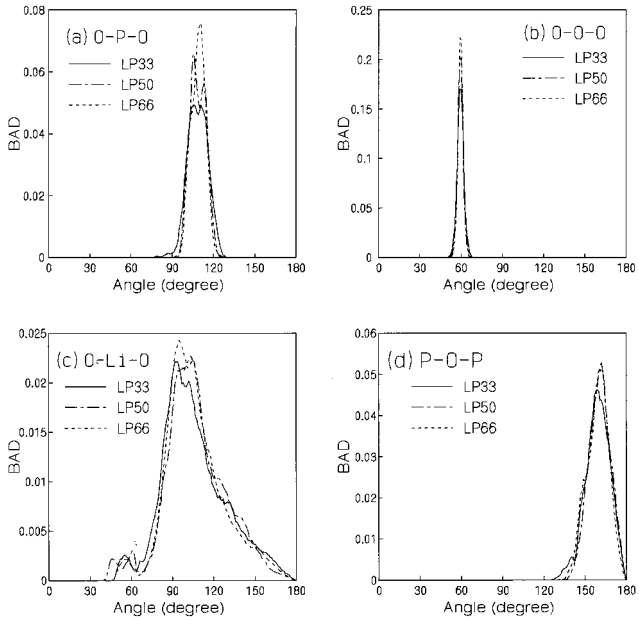

Figure 2. Bond angle distributions (BAD) at 300 K for the three glasses: (a) O—P—O; (b) O—O—O; (c) O—Li—O; and (d) P—O—P.

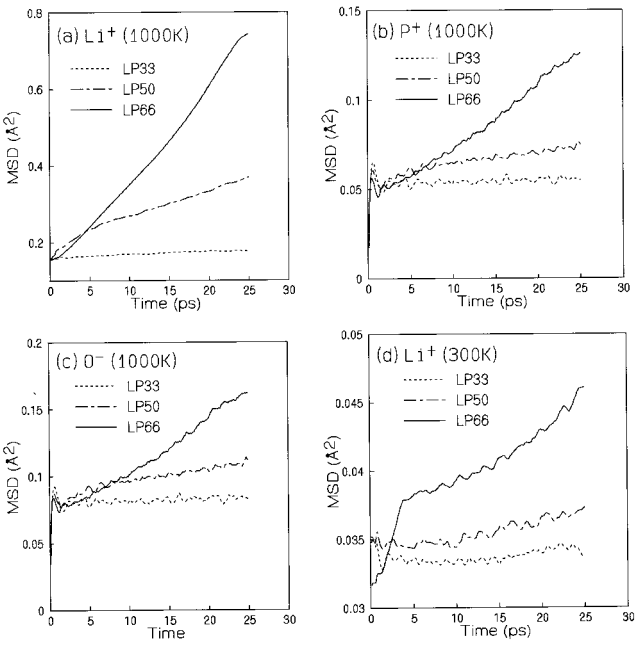

Figure 3. The mean square displacement (MSD) determined at 1000 K for the glasses: (a) Li^+ ions; (b) P^+ ions; (c) O^- ions; and (d) MSD of Li^+ ion at 300 K.

distances are in agreement with the experimental P—O distances of 1.46 and 1.62 Å observed in crystalline phosphates.[20,21] On this basis and on the basis of previous extended X-ray absorption fine structure (EXAFS) results on phosphate glasses,[22] the short P—O distance has been associated with NBOs and the long P—O distance with BOs. It is seen in Table 2 that the sum of the numbers of coordinating BOs and NBOs is close to 4.0 in all the compositions. The O—P—O bond angles (Figure 2a) have a very narrow distribution, with the peak value close to 109° in LP66 glass. In both LP33 and LP50, the BAD peak is split and the midpoint at half maximum is close to the tetrahedral angle of 109°48' in both cases. The absence of splitting in the case of LP66 may be attributed to the presence of only pyrophosphate units in which P is connected to three short bonds (one double bond and two NBOs) and one long bond (see later). This absence of splitting results in one dominant O—P—O peak into which the other O—P—O peak has merged. The O—O—O BAD is even narrower than the O—P—O BAD and peaks close to 60°. The oxygen coordination number of 4.0 together with the O—P—O and O—O—O BADs confirm the tetrahedrality of the phosphate species in the glass, and the presence of two well-defined P—O peaks confirm the presence of BOs and NBOs connected to phosphorus atoms in the structure.

The PDF of Li—O [Figure 1(c)] indicates the presence of a well-defined first neighbor environment of oxygen atoms around Li^+ ions. The Li—O distance beyond the first neighbors appears rather spread out. The number of oxygen atoms coordinated to lithium suggests a pronounced tendency of Li^+ ions to acquire a tetrahedral coordination in phosphate glasses. The observed coordination number is, however, always <4.0. That the coordination of Li^+ ions may be tetrahedral is also suggested by the O—Li—O BAD [Figure 2(c)], which peaks around 100° and is close to the tetrahedral angle.

The P—O—P BAD shown in Figure 2d is narrow and peaks around 160°, indicating a tendency towards formation of well-defined intertetrahedral orientations. The P—P coordinations are low and close to the ideal value of 2 expected for long metaphosphate chains in LP50 composition. It may be seen from Table 2 that the Li—Li coordination (second shell) number increases significantly from LP33 (2.2) to LP66 (6.2). However, the Li—Li—Li BAD did not reveal any feature to suggest the presence of cation structural motifs. Presence of peaks around 60° and 110° in the BAD have also been noted, and they can be attributed to a possible tetrahedral Li—Li coordination. Because Li—P coordinations at similar second neighbor distances are also tetrahedral, the two (Li with Li and P) coordinations may together constitute the complementary (interpenetrating) tetrahedra present in a cubic coordination shell of Li and P atoms around a given lithium atom.

The P—O PDF was analyzed further by measuring the areas under the twin peaks corresponding to NBO (short) and BO (long) distances. The ratio of the areas (coordination numbers) representing the NBO/BO ratio are 0.61, 0.92, and 1.68, respectively, for LP33, LP50, and LP66. The expected values of NBO/BO ratios based on simple modification scheme are 0.6, 1.0, and 1.4, respectively, for LP33, LP50, and LP66. The latter values have been calculated assuming that P═O is a short bond and structurally (not chemically) equivalent to NBO and therefore indistinguishable from the latter. Therefore, the agreement in the NBO/BO ratio between calculated values and those obtained by PDFs may be considered rather satisfactory. The somewhat higher difference between the calculated and observed (from MD) NBO/BO ratio in the case of LP66 can be attributed to the increased inadequacy of the potential parameters for this extreme glass-forming composition. We have performed the structural analysis just presented with simulation data obtained at 700 and 1000 K also, and the results were very similar. As noted earlier, the structural findings from MD simulation remain unaffected when a potential function based on full charges ($Li:1^+$, $P:5^+$, and $O:2^-$) are used along with appropriate repulsive parameters. In summary, the static structural information obtained from the present simulation is in good agreement with experimental results and the now traditional description of the alkali phosphate glass structures.

Dynamic Properties of Simulated Glasses. The Li^+ ion motion was examined by computing the mean square displacements (MSDs), which are shown in Figure 3a for the three compositions at 1000 K. It is evident that there is a remarkable increase in MSD with increase in modification (*R* value). The MSDs of both phosphorous and oxygen (Figures 3(b) and 3(c)]

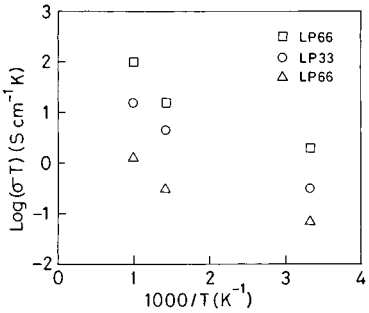

Figure 4. Arrhenius plots of lithium ion conductivity (obtained using diffusion coefficients and Nernst−Einstein relation).

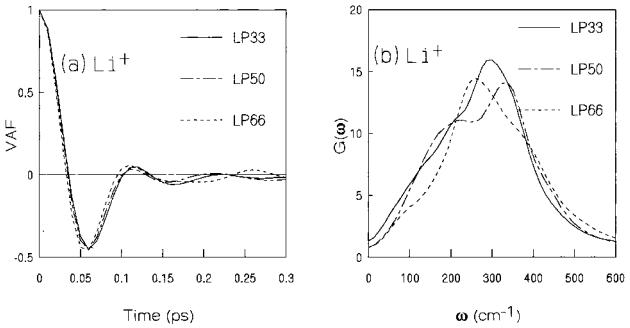

Figure 5. (a) Velocity autocorrelation function (VAF) and (b) corresponding power spectra $G(\omega)$ of lithium ions at 300 K.

are significantly lower than that of Li^+ ions, even at 1000 K. We therefore assumed that P and O atoms (phosphate) in the matrix remain immobile and only Li^+ ions contribute to ion transport. To examine if reasonable transport parameters can be obtained from the present simulation, MSDs were determined at both 700 and 300 K. The MSDs of Li^+ ions at 300 K are shown in Figure 3(d). The data collected at 300 K were insufficient to give satisfactory statistics for the evaluation of the MSD of Li^+ ions because much longer computational times were needed than those used here. Diffusion coefficients (D) were, however, obtained from the slopes, and the corresponding conductivities (σ) were calculated by the Nernst−Einstein relation $\sigma = Nq^2D/kT$, where N is the number concentration of mobile Li^+ ions. Lithium ion conductivity at 1000 K was 1.3×10^{-3}, 1.6×10^{-2}, and 9.9×10^{-2} S cm^{-1}, respectively, for LP33, LP50, and LP66 glasses, and these values are much higher than the experimentally known values.[6] The conductivities at different temperatures are shown in Figure 4 in Arrehenius plots. Because the statistics of MD data were more satisfactory at the higher temperatures, the activation barriers (E_a) were determined using the σ values at two higher temperatures only. The activation barriers were 0.29, 0.25, and 0.37 eV for LP33, LP50, and LP66, respectively, which are significantly lower than experimental values.[6]

One of the reasons for the high conductivities and low activation barriers of the simulated glasses may be that the simulated glasses correspond to high fictive temperatures.[17,18] Therefore, it is difficult to make quantitative comparisons of the results obtained from MD simulations with those from experiments. In the case of LP50, the experimental conductivity at 423 K is $\sim 10^{-4}$ S cm^{-1}, whereas for the simulated glass, the conductivity even at 300 K is 10^{-3} S cm^{-1}. Both the activation barriers and conductivities of the simulated glasses are significantly different from those found experimentally when they are calculated from MSD data by the Nernt−Einstein equation. This difference is because of the lack of validity of such a procedure. The situation is much improved by adopting an alternate approach that is discussed later.

The velocity autocorrelation functions (VAFs) of all the three ions were examined at all the temperatures, and those for Li^+ ions are shown in Figure 5(a). For phosphorus and oxygen, the first negative dip in VAF was rather insignificant and the correlation almost vanished in <0.5 ps. However, the Li^+ ions exhibited the first negative hump in VAF, as shown in Figure 5(a). The correlation function beyond the hump consisted of highly damped oscillations that vanished around 0.5 ps. The power functions at 300 K are shown for all the three compositions in Figure 5(b). The major peak at 9×10^{12} s^{-1} (300 cm^{-1}) may be compared with cage vibrational frequency of Li^+ ions in oxygen cages. The cage vibrational frequency of the simulated glasses appears to be lower compared with those from experiments (in the case of LP50 the experimental value reported by Exarhos et al.[23] is 420 cm^{-1}). As simulation results, these frequencies may be considered as reasonably satisfactory. It is interesting to see that the power spectrum actually consists of at least two other major frequencies convoluted into the main absorption as shoulders. The low frequency peaks have been observed in far infrared (IR) experiments also and have been examined extensively in a variety of glasses by Kamitsos et al.[24,25]

In earlier studies on silicate and molybdate glasses[17,18] it was found that satisfactory activation barriers for ion transport are obtained by making use of jump frequencies (ν_j) of the ions obtained directly along with cage vibrational frequency (ν_o, from VAF data) in the expression $\nu_j = \nu_o \exp(-E_\nu/kT)$. The parameter was evaluated by this procedure using the jump frequency data in the case of LP66 glass. The average number of jumps of Li^+ ions in 50 ps was evaluated for the entire ensemble. Lithium ion displacements were considered as jumps whenever such displacements equal or exceed the lowest Li−Li distance given in Table 2. The parameter ν_j was thus found to be 4.55×10^{10} for LP66 at 1000 K. Using the expression just presented together with ν_o of 9×10^{12} (from VAF data), E_ν was found to be 0.46 eV. This value of E_ν is much closer to the experimental direct current (dc) activation barrier of 0.55 eV. This curious difference in the estimated activation barriers using two different approaches needs to be examined further. It is also important to know what barrier is being calculated by these procedures.

MSD, as evaluated in MD simulations, does not stipulate that Li^+ ions should not return to the site of origin, which would be difficult in simulations of glasses at high temperatures because the local structures can keep changing. The observed MSD actually conceals all the information regarding the to-and-fro motion of Li^+ ions between nearest pairs of sites. These jumps are in the nature of correlated hops. During the 25 ps used for determining MSD, the Li^+ ions would have performed several such correlated jumps from their sites because the vibrational frequency of the Li^+ ions is of the order of terahertz (THz). If a good proportion of such jumps were uncorrelated, then the value of MSD ought to have been much greater. Because MSD is only 0.7 Å^2, either a tendency for nondiffusion or of highly correlated jumps of Li^+ ions between pairs of sites is suggested. We favor the latter possibility. The activation barrier is calculated using the relation between ν_j and ν_o and would therefore largely reflect the barrier experienced by Li^+ ions during the correlated jumps. The barrier so obtained represents the alternating current (ac) conductivity barrier. The value of 0.46 eV is indeed close to (βE_{dc}), with a β value of 0.7 and the experimental $E_{dc} = 0.55$ eV, which is as expected from the mode coupling model.[26] However, it is not clear why the activation barriers evaluated using MSD data together with Nernst−

TABLE 3: P^n Units Present in the System in Percentage (%)

composition	temperature (K)	P^0	P^1	P^2	P^3	P^4
LP33	300	0	6	41	47	6
	700	0	4	41	47	8
	1000	0	4	39	49	8
LP50	300	0	18	50	31	1
	700	0	16	54	29	1
	1000	0	14	57	28	1
LP66	300	7	39	45	9	0
	700	3	40	47	10	0
	1000	6	44	46	4	0

Einstein relation are significantly lower. This result could be the consequence of limited validity of the use of Nernst−Einstein relation for the evaluation of the conductivities in MD simulations.

NBO−BO Dynamics. We now address the problem of the dynamics of NBOs in phosphate glasses using the present simulation data. This investigation was accomplished by first identifying the various phosphate species (P^n) present in the glasses. It may be noted that P^n is the phosphate species in which n BOs are attached to the central P atom. This step was followed by the observation of $P^n \rightarrow P^{n'}$, where $n \neq n'$ and n and n' are both ≤ 4. Species with $n = 4$ have no corresponding structural unit in real glasses, unless one of the oxygen atoms connected to phosphorous by double bond is converted to a single bond as happens in lead oxide-containing phosphate glasses.[27] The species P^o represents an orthophosphate unit. However, it will be seen shortly that the number of P^n with extreme values of n found in simulated glasses is very low. Using the P—O distance criterion and the oxygen coordination number of P atoms, the various P^n species were identified and counted after every 100 fs. These numbers were averaged over a total simulation time of 50 ps. We consider 100 fs as a convenient time window because it is only slightly higher than the vibrational time scales and far higher than the jump times of Li^+ ions. Also, it was ensured that by not using longer than 100 fs time windows, the $P^{n'} \rightarrow P^n$ re-conversions were insignificantly low. Still shorter time windows were not necessary. The number of P^n increases linearly up to 100 fs time windows and the slope of its variation begins to decrease above that, indicating that re-conversions are becoming significant above 100 fs. Because the data were collected for 50 ps, 500 time slots were available for averaging, which provided good statistics of P^n species present in the system. These results are given in Table 3 for three compositions at three different temperatures. It may be noted that the P^o species is absent in LP33 and LP50, whereas P^4 is absent in LP66. But both P^o and P^4 are only 8% or less in any of the compositions.

A check on the internal consistency of P^n data was performed in conjunction with the data in Table 1. The total charge on P^n was evaluated using the expected charge on each type of P^n species (charge on P^n is the sum of charges on all the atoms in P^n). This value must balance against the total charge of Li^+ ions in the system. For example, in the case of LP33 at 1000 K, the total negative and positive charges are −53 and +56, respectively. The small disparity in the net negative charge on the P^n species and the positive charge on the Li^+ ions is because of the small uncertainty in the designation of oxygen atoms as NBO or BO based on the distance criteria obtained from Figure 1(a) in which the BO/NBO peaks are not clearly separated. The region of overlap of the higher and lower cutoff of the NBO and BO peaks, respectively, renders the accounting of oxygens and hence of charge on P^n slightly arbitrary. However, the system as a whole remains electrically neutral because such a criterion is built into the simulation procedure.

TABLE 4: Average Number of Flips Seen in 100 fs and Flip Frequency and Its Activation Energy (E_f)

composition	300 K	700 K	1000 K	E_f (eV)
number of flips				
LP33	9	16	21	
LP50	6	14	20	
LP66	9	15	21	
flip frequency (10^{11} s^{-1})				
LP33	4.74	8.35	11.2	0.030
LP50	1.81	4.46	6.27	0.044
LP66	1.72	3.03	4.3	0.031

TABLE 5: $P^n \leftrightarrow P^{n'}$ Transformations Averaged for 100 fs in Percentages (%)

composition	temperature (K)	$P^0 \leftrightarrow P^1$	$P^1 \leftrightarrow P^2$	$P^2 \leftrightarrow P^3$	$P^3 \leftrightarrow P^4$	others
LP33	300	0	34	29	33	4
	700	0	28	26	41	5
	1000	0	27	29	39	5
LP50	300	0	44	41	9	6
	700	0	46	39	9	6
	1000	0	46	37	10	7
LP66	300	39	8	50	0	3
	700	22	24	48	0	6
	1000	13	58	21	0	8

The focus of interest in the present investigation was the evaluation of the life times of the P^n units, so the transformation $P^n \rightarrow P^{n'}$ was examined for each and every P^n unit after every 100 fs time step. The same distance criteria as earlier were used in identifying $P^{n'}$. The time dependence of the transformation of P^n units was thus assessed at the end of every successive 100 fs and the various $P^n \rightarrow P^{n'}$ transformation data were accumulated for a total time of 50 ps. The data were averaged for 100 fs. In Table 4, such averages of $P^n \rightarrow P^{n'}$ transformations are summarized for the three glasses at three different temperatures. In all cases, the number of $P^n \rightarrow P^{n'}$ was numerically almost equal to $P^{n'} \rightarrow P^n$ for the same values of n and n'. We have therefore grouped them as $P^n \leftrightarrow P^{n'}$ in Table 5, and the numbers are given as percentages for all types.

From the data in Table 5 we note that every P^n species has changed to some $P^{n'}$, but $P^n \leftrightarrow P^{n\pm1}$ accounts for the largest number of changes. The entries in the column headed 'others' includes such occasional transformations as $P^n \leftrightarrow P^{n\pm2}$ and $P^n \leftrightarrow P^{n\pm3}$, and their percentages are very small. In the composition LP33 (which is an ultraphosphate composition), $P^3 \leftrightarrow P^4$ transformations are the most significant, whereas in the composition LP66 (a mixture of meta- and pyrophosphates), the highest percentage of transformations are the $P^0 \leftrightarrow P^1$ (ortho ↔ pyro) type. But it must be noted that both P^0 and P^4 account for only a small percentage of the equilibrium species (refer to Table 4) and therefore are seen as transient species contributing most to the observed bond transformations.

The $P^n \leftrightarrow P^{n+1}$ transformations are in a sense NBO−BO transformations. Because of the charge neutrality of the system, the results also imply that $P^n \rightarrow P^{n+1}$ conversion is compensated by some $P^{n'} \rightarrow P^{n'-1}$ conversion. The transformation therefore is essentially a BO−NBO bond flip. Thus, the average of $P^n \leftrightarrow P^{n'}$ conversions in Table 4 correspond to twice the number of bond flips (twice because BO−NBO and associated charge conserving NBO−BO flips have been counted as independent events). We thus have a count of the total number of bond flips that occurs in 100 fs (obtained from averaging over 50 ps). The frequency of bond flips (ν_f) can therefore be calculated by dividing total

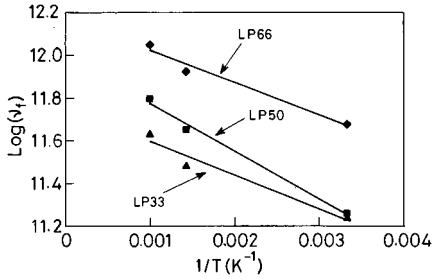

Figure 6. Bond flip frequency (ν_f) for the three glass compositions as a function of inverse temperature (Arrhenius plots).

average number of flips by the time taken (100 fs). The ν_f data for all the glasses are given in Table 4. The numbers suggest that the bond flip frequency (ν_f) increases with temperature. The variation of $\log(\nu_f)$ as a function of $1/T$ is shown (Figure 6) in an Arrhenius plot, and activation barriers obtained for the bond flip processes are listed in Table 4.

The information in Table 4 is most revealing. First of all, the flip frequencies are very high, yet much lower than the vibrational frequencies. The activation barriers are of the order 0.04 eV (~5 kJ/mol), which is surprisingly of the same magnitude as predicted by Greaves and Ngai[14,15] for the bond flip process. The phosphate glasses can therefore be viewed as a phosphate network in which oxygen atoms are of both BO and NBO type with BO−NBO bond flipping occurring at very high frequencies. Nevertheless, a constant NBO-to-BO ratio is maintained for electrical neutrality. The Li^+ ion jump frequencies (ν_L) calculated from the MSD data at 1000 K are several orders of magnitude lower than ν_f. However the ν_j values (ν_j should be ideally equal to ν_{Li}) determined by the direct examination of the jumps in LP66 glass at 1000 K are of the order 4.55×10^{10} Hz. Even this value is an order of magnitude lower than ν_f. Because the activation barriers for bond flipping are much lower than the activation barriers for Li^+ ion jumping the difference between ν_j and ν_f becomes much higher at lower temperatures. Therefore, the results clearly indicate that NBO−BO bond flips and Li^+ ion jumps may not be strongly coupled processes. Correspondingly, the activation barriers for ν_f and ν_j are very different.

Lithium Ion Migration in Relation to NBO Concentration. Lithium ion dynamics may still involve NBOs for a different reason. The migration of Li^+ ion may be associated with the presence of some optimum number of NBOs in the first coordination of Li^+ ions. Such congregation (a high concentration) of NBOs may occur as statistical events during bond flips, and the frequency of occurrence of such events may correspond to Li^+ ion jump frequencies (ν_j). To investigate this aspect in more detail, the number of NBOs surrounding the Li^+ ions were determined. Because the computational statistics are significantly better at 1000 K and also because the MSD, of Li^+ ions are reasonably high only at that temperature, this computation was performed at 1000 K. The results, given in Table 6, indicate that most (highest percentage) of the Li^+ ions are surrounded by only three NBOs, although the oxygen coordination number for Li^+ ions is close to four.

The site energies of the Li^+ ions surrounded by different numbers of NBOs were also evaluated and are given in Table 6. The three NBO coordinated sites have the least negative energies. Therefore, an environment consisting of three NBOs appears to be optimal in terms of energy. The presence of NBOs lifts the Li^+ ions from the bottom of their potential well. Assuming that the saddle point energies of the Li^+ ion are not much affected during bond flips, such elevation of the Li^+ ion site energy is equivalent to a reduction of activation barrier for its site-to-site jumps. Therefore, only such Li^+ ions may contribute most to Li^+ ion transport or, in this sense, Li^+ ion jumping is NBO assisted.

TABLE 6: Lithium Ion Population (in Percentage %) in Different Li−NBO Coordination, and Their Site Energies and Jumps Seen at 1000 K

	number of NBO around lithium ion				
composition	1	2	3	4	5
percentage of Li^+ ions					
LP33	7	31	47	15	0
LP50	5	27	50	18	0
LP66	12	27	38	19	4
Site Energy (eV)					
LP33	8.98	8.94	8.35	8.52	
LP50	9.22	9.08	8.48	8.51	
LP66	10.65	9.51	8.69	8.74	8.82
lithium ion iumps					
LP66	291	223	412	339	92

The Li^+ ion jumps have been further examined in relation to the number of NBOs in their coordination. These jumps have been listed for each category in Table 6. It is clearly seen that indeed Li^+ ions in the optimal energy environments jump the most.

The rather high bond flip frequencies observed here is very curious. If the bond flips propagate through the glass structure so as to involve all the P^n species present in a glass composition with such a high frequency, all the P^n species would become indistinguishable in the NMR time scale and give rise to single resonance. This occurence would be inconsistent with the fact that several P^n NMR resonances are observed in experiments.[29] However, when Tables 4 and 1 are examined together closely, we note that only a small fraction of all the species (total phosphorus atoms) are involved in bond switching transformations. Bond switching may be confined to a small region around these phosphorus atoms only. A large fraction of the P^n species may therefore not be chemically affected by the bond switching. It is possible that bond switching is occurring in the manner of back and forth, $P^n \leftrightarrow P^{n+1}$ conversions at the observed fast rates at these few centers. It is expected that such coupled pairs of P^n species produce a resonance at average chemical shift values. Because their percentage is small and the chemical shifts of different P^n species are fairly close, the effect may manifest as a broadening of P^n resonances in NMR. In fact, in the NMR work of Alan and Brow[28] on alkali phosphate glasses, a significant overlapping of P^n resonances is evident even at spinning speeds of 12.5 kHz. These authors have also noted off-diagonal intensities in two-dimensional NMR of these glasses, even for zero delay times. Although Alan and Brow[28] have attributed the off-diagonal intensities to the dipolar interactions involving ^7Li, we suggest that it arises from the fast $P^n \leftrightarrow P^{n+1}$ exchanges.

The fast kinetics of BO−NBO switching in these phosphate glasses is very dissimilar to the kinetics seen in silicate glasses. We wish to examine the possible origin of this feature. In phosphate glasses the maximum coordination of phosphorus is 4, but its connectivity in the glass structure is only 3. Above a certain level of modification, the NBO and P═O become structurally indistinguishable.[29,30] Such indistinguishability is suggestive of ready rehybridization and electron density redistribution on singly connected oxygens, which we feel enables NBO-type oxygens on a given phosphorus atom to establish link with neighboring phosphate tetrahedra as a first step towards BO−NBO conversion. We visualise the conversion step to

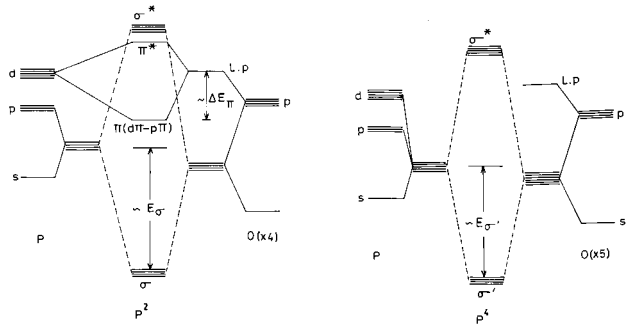

Figure 7. Molecular orbital schematic for the ground (P^2) and excited (P^4) states (see text).

involve the following scheme:

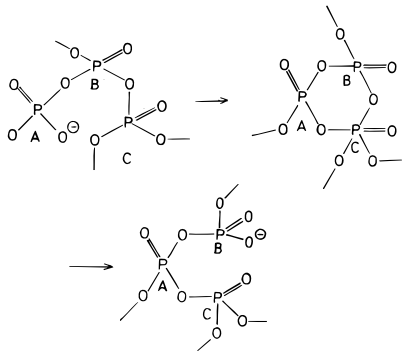

$$P^2 + 2P^3 \longrightarrow 2P^3 + P^5 \longrightarrow 2P^3 + P^2$$

$$(P{:}\,A) + (P{:}\,B + P{:}\,C) \longrightarrow (P{:}\,A + P{:}\,B + P{:}\,C) + (P{:}\,A + P{:}\,C) + (P{:}\,B)$$

The activated state for phosphorus labeled *B* can presumably be a trigonal bipyramid (TBP). This geometry is well known in phosphorus chemistry and therefore constitute a facile low-energy activated state. That the activated state may not be of high energy is further illustrated by the schematic molecular orbital diagram shown in Figure 7 for the initial (also the final; 4 coordinated phosphorus atoms only) and the excited states (which contains a 5 coordinated phosphorus species). These species are the only relevant ones for a discussion of energetics.

In the P^2 species, the $p\pi-d\pi$ interaction is shown with energy (ΔE_π) that corresponds to the energy gain by the π-bond formation. The activated P^4 state is assumed to be a trigonal bipyramid (TBP) in which all five P—O bonds are assumed to be equivalent (an approximation). The creation of the five sp^3d hybridized orbitals on phosphorus costs additional energy equal to the difference between the p and the d orbital energies on phosphorus. The formation of five equivalent bonds leads to an energy gain that is roughly equal to one P—O bond energy in the activated TBP. The P—O single bond energy in TBP may not be very different from average P—O bond energy in the initial (ground state) P^2 species. However, the $p\pi-d\pi$ interactions are absent in the P^4 species. Thus, from the schematic in Figure 7, the net activation barrier for the process corresponds to $(5E_{\sigma'} - 4E_\sigma - \Delta E_\pi)$ where $E_{\sigma'}$ and E_σ are the σ bond energies in the TBP and tetrahedral phosphate species, respectively. This energy is most likely to be small because, in essence, the same orbitals are involved slightly differently in bonding in both the species.

It is therefore evident that in phosphates, such $P^2 - P^4$ changes can occur primarily because of the relatively ready d-orbital participation in bonding. Furthermore, the bond switching requires that a P^2 species be adjacent to a diad of P^3 species (as visualized in the preceding scheme). In fact, the two-connected P^2 species can swing on the O—P—O bond segment towards one of the P^3 units in the neighboring diad and initiate the aforementioned switching. This swinging or the libratory motion makes the NBO on P^2 "bang" onto the phosphorus in the P^3 species, providing very frequent opportunities for the activation to occur. The success rate of the reaction is therefore close to the librational frequencies that can be of the order 10^{11} Hz, which is consistent with the observation in the present simulation. Facile participation of d orbitals in bonding is therefore considered as the underlying reason for the observed fast bond switching kinetics. The situation in silicates is likely to be more complex, leading to quantitative differences.

It has not been possible to assess if the BO—NBO dynamic results just presented are heavily dependent on the potential parameters we have used. There is no a *priori* reason to believe that the results would be qualitatively different. Therefore, the Li^+ ion motion is not entirely indifferent to the NBO environment, although we may have to substitute the 'catch and carry' image of Ingram[12] with a different similitude.

The NBO—BO dynamics have implications on current models of transport. For example, the assumption regarding the presence of local minima around an NBO loses significance because of the high frequency of NBO—BO flips. There is, indeed, a multiplicity of the types of sites created by the bond flips, with different energies, indicating that Li^+ ions can have a spectrum of distinct jump frequencies. This result affirms the presence of a non-Debye relaxation that is manifest in all frequency-dependent measurements.

It is important to note that phosphate glasses are quite representative of a whole class of glasses based on the presence of network formers and modifiers. Therefore, NBO—BO statistics, their interconversion dynamics, and their influence (or lack of it) on cation motion can be expected to be qualitatively similar to those found in the present studies.

Conclusions

The presence of two different oxygen coordinations corresponding to BO and NBO has been borne out in MD simulation of lithium phosphate glasses. The modifying effect of lithium oxide and the formation of different phosphate P^n units has been ascertained. Various structural and dynamic properties of lithium phosphate glasses have been reasonably well simulated. The dynamics of NBOs leads to transformations of phosphate units, $P^n \leftrightarrow P^{n'}$ ($n \neq n'$). The Li^+ ion jump frequencies are far less than the frequency of NBO—BO bond flips. It is suggested that the Li^+ ion migration and bond flips are not directly coupled. However, the statistics of NBOs around Li^+ ions, and the site energies and jumps of Li^+ ions have indicated the presence of an optimal NBO environment that favors Li^+ ion migration.

Acknowledgment. The simulations were carried out using the SGI-CRAY (J916/128-8) facility of the MASTER laboratory, ENSCPB, and the authors are grateful to the authorities. The authors thank European Commission for financial support of this research. Helpful discussion with Dr. N. Baskaran is warmly acknowledged.

References and Notes

(1) Van Wazer, J. R. *Phosphorus and its Compounds*; Interscience: New York, 1958; Vol. I.

(2) Martin, S. W. *Eur. J. Solid State Inorg. Chem.* **1991**, *28*, 163.

(3) Brow, R. K.; Kirkpatrick, R. J.; Turner, G. L. *J. Non-Cryst. Solids* **1990**, *116*, 39.

(4) Prabakar, S.; Rao, K. J.; Rao, C. N. R. *Chem. Phys. Lett.* **1987**, *139*, 96.
(5) Prabakar, S. Ph.D Thesis, Indian Institute of Science, Bangalore, 1991.
(6) Martin, S. W.; Angell, C. A. *J. Non-Cryst. Solids* **1986**, *83*, 185.
(7) Pantano, C. G. *Experimental Techniques of Glass Science*; Ed. Simmons, C. J., El-Bayoumi, O. H., Eds.; The American Ceramic Society: Westerville, OH, 1993; p 129.
(8) Stebbins, J. F.; Oglesby, J. V.; Xu, Z. *Am. Mineral.* **1997**, *82*, 1116.
(9) Dirken, P. J.; Kohn, S. C.; Smith, M. E.; van Eck, E. R. H. *Chem. Phys. Letts.* **1997**, *266*, 568.
(10) Ravaine, D.; Souquet, J. L. *Phys. Chem. Glasses* **1977**, *18*, 27.
(11) Ravaine, D.; Souquet, J. L. *Phys. Chem. Glasses* **1978**, *19*, 115.
(12) Bunde, A.; Funke, K.; Ingram, M. D. *Solid State lonics* **1996**, *86*, 1311.
(13) Greaves, G. N.; Ngai, K. *Phys. Rev. B* **1995**, *52*, 6358.
(14) Greaves, G. N.; Ngai, K. L. *J. Non-Cryst. Solids* **1994**, *172*−*174*, 1378.
(15) Farnan, I.; Stebbins, J. F. *J. Am. Chem. Soc.* **1990**, *112*, 32.
(16) Ingram, M. D. *Curr. Opin. Solid State & Materials Sci.* **1997**, *2*, 399.
(17) Balasubramanian, S.; Rao, K. J. *J. Non-Cryst. Solids* **1995**, *181*, 157.
(18) Karthikeyan, A.; Rao, K. J. *J. Phys. Chem. B* **1997**, *101*, 3105.
(19) Allen, M. P.; Tildesley, D. J. *Computer simulation of liquids*; Clarendon: Oxford, 1987.
(20) Corbridge, D. E. C. *Acta Crystallogr.* **1956**, *9*, 308.
(21) MacArthur, D. M.; Beevers, C. A. *Acta. Crystallogr.* **1957**, *10*, 428.
(22) Dalba, G.; Fornasini, P.; Rocca, F.; Lagarde, P.; Vlaic, G. *J. Non-Cryst. Solids* **1988**, *106*, 181.
(23) Exarhos, G. J.; Miller, P. J.; Risen, W. M., Jr. *J. Chem. Phys.* **1974**, *60*, 4145.
(24) Kamitsos, E. I.; Chryssikos, G. D.; Karakassides, M. A. *Phys. Chem. Glasses* **1988**, *29*, 121.
(25) Kamitsos, E. I.; Chryssikos, G. D. *Solid State lonics* **1998**, *105*, 75.
(26) Ngai, K. L.; Martin. S. W. *Phys. Rev. B* **1989**, *40*, 10550.
(27) Selvaraj, U.; Rao. K. J. *J. Non-Cryst. Solids* **1988**, *104*, 300.
(28) Alam, T. M.; Brow, R. K. *J. Non-Cryst. Solids* **1998**, *223*, 1.
(29) Suzuki, M.; Ueno, M. *J. Phys. (Paris)* **1985**, *261*, 28.
(30) Hoppe, U.; Walter, G. *Z. Naturforsch* **1996**, *51a*, 29.